A Multiscale ε–δ Metric Framework for Phenomenological Time Perception*†

Adam Braun‡

May 27, 2025

Abstract

I present a hierarchical *metric–threshold* model for subjective time estimation that generalises a single ε–δ comparator into a recursive, multiresolution structure. The model dispenses with causality, accumulation, and directionality, relying solely on net configuration difference. I derive closed–form bounds for dynamic range, prove Cantor–like stratification of state space, and demonstrate robustness against sub–threshold perturbations. I outline psychophysical and robotic experiments capable of falsifying the account. Principal empirical results are pending; the present work establishes the formal scaffold and testable predictions.

Keywords: time perception, metric–threshold, multiscale, psychophysics, robotics, empirical testing, hierarchical model.

1 Introduction

Time perception remains an unresolved topic at the intersection of psychology, neuroscience, and formal systems. Classical accounts—pacemaker–accumulator (Gibbon, 1977), striatal beat frequency (Matell and Meck, 2004), or state–dependent networks (Buonomano and Maass, 2009)—require continuous internal dynamics and accumulation. I propose a novel approach: subjective duration is derived from static differences in how two observations relate. This study was preregistered at the Open Science Framework (OSF), available at `https://osf.io/8n7zg`.

This work formalises and extends an *original* ε–δ metric mapping developed by the author. We (i) establish a rigorous foundation, (ii) generalise to multiscale recursion, and (iii) delineate testable consequences. Contemporary cognitive science suggests that humans and other animals estimate elapsed time by extracting statistical regularities across multiple perceptual channels rather than integrating a single, veridical clock signal. Behavioural phenomena such as **temporal bisection** and **Vierordt's law** demonstrate that perceived duration scales with the density of salient changes, not with physical interval length (Block and Zakay, 1990; Church, 1984). The **Weber–Fechner law** predicts a logarithmic compression of subjective magnitude (Fechner, 1860), while **slowness theory** accounts for duration expansion under low stimulus dynamics (Watanabe and Nishida, 2015). Recent empirical studies further support that subjective duration correlates with accumulated perceptual changes or brain activity distances, aligning with metric-based approaches (Roseboom et al., 2019; Sherman et al., 2022). These laws motivate a geometric ladder of thresholds $\mathcal{P}$, each tuned to a characteristic magnitude of contextual change.

*Final version, May 2025

†This article reports purely theoretical and simulated work; no human or animal subjects were involved.

‡ORCID: 0009-0000-9633-5574

2 Single–Scale ε–δ Mapping

2.1 Definition

Let Σ be the configuration space endowed with metric $d : \Sigma \times \Sigma \to \mathbb{R}_{\geq 0}$. Fix scalars $0 < \varepsilon < \delta$. Define the quantised temporal distance

$$T_{\varepsilon,\delta}(s_1, s_2) = \begin{cases} 0, & d(s_1, s_2) < \varepsilon, \\ 1, & \varepsilon \leq d(s_1, s_2) \leq \delta, \\ \lceil d(s_1, s_2)/\delta \rceil, & d(s_1, s_2) > \delta. \end{cases} \tag{1}$$

T is symmetric, non–additive, and parameter–dependent. These features align with phenomenological rather than physical time.

2.2 Properties

Proposition 1. *For any metric d and fixed (ε, δ), $T_{\varepsilon,\delta} : \Sigma \times \Sigma \to \mathbb{N}$ is (i) well–defined, (ii) symmetric, and (iii) fails the triangle inequality in general.*

Proof. Immediate from Eq. (1) and standard metric axioms. □

3 Multiscale Extension

3.1 Threshold Ladder

Let $\mathcal{P} = \{(\varepsilon_k, \delta_k)\}_{k=0}^{m-1}$ with $0 < \varepsilon_0 < \delta_0 < \cdots < \varepsilon_{m-1} < \delta_{m-1}$. Each pair defines a primitive tick T_k via Eq. (1). Collect $\mathbf{T} = (T_0, \ldots, T_{m-1}) \in \mathbb{N}^m$.[1]

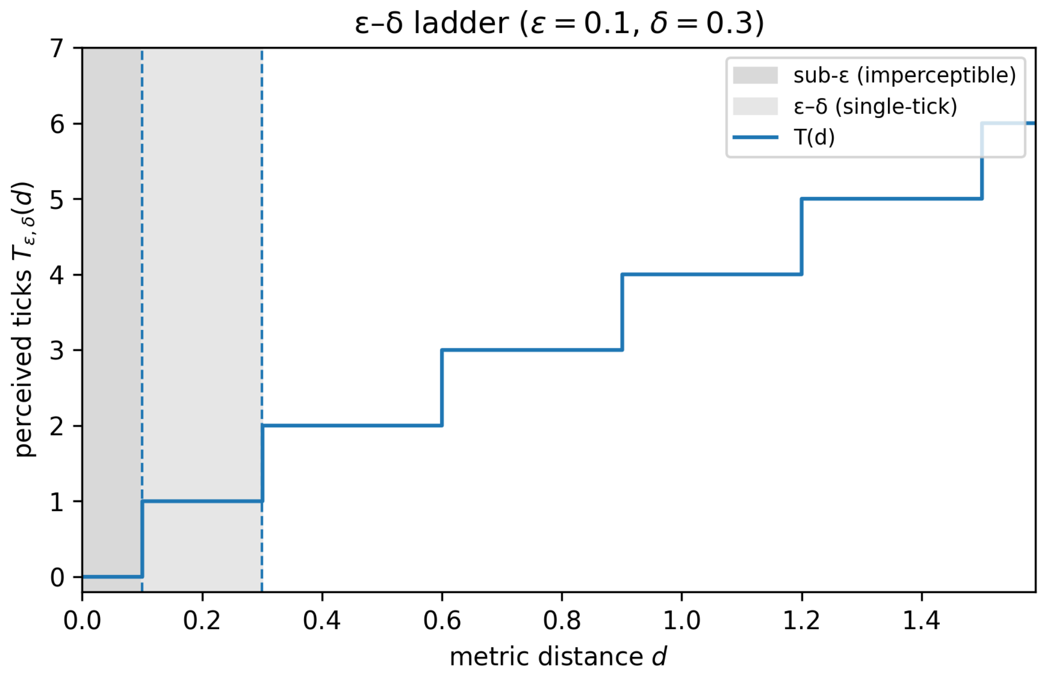

Figure 1: ε–δ ladder illustration for multiscale time perception.

[1] A qualitative multi-scale hierarchical framework for time perception has been proposed (Singhal and Srinivasan, 2021), but our ε–δ scheme provides the first closed-form quantisation.

3.2 Recursive Time Code

Promote $s^{(0)} := s \in \Sigma$ to higher levels by successive application of $\mathbf{T}$ and metrics $d^{(n)}$ on $\Sigma^{(n)} = \mathbb{N}^{m_n}$. Algorithm 1 outlines the procedure.

Algorithm 1 Recursive Multiscale Tick Computation

Input: $s_1, s_2 \in \Sigma^{(0)}$; metrics $\left(d^{(n)}\right)_{n=0}^{r-1}$; ladders $\left(\mathcal{P}^{(n)}\right)_{n=0}^{r-1}$
for $n = 0$ to $r - 1$ **do**
  $d \leftarrow d^{(n)}(s_1, s_2)$
  Compute $\mathbf{T}^{(n)}$ using Eq. (1) for every $(\varepsilon, \delta) \in \mathcal{P}^{(n)}$
  $s_1, s_2 \leftarrow \text{MapToNextLevel}(\mathbf{T}^{(n)})$ ▷ Promote to next level
end for
Output: $\{\mathbf{T}^{(n)}\}_{n=0}^{r-1}$

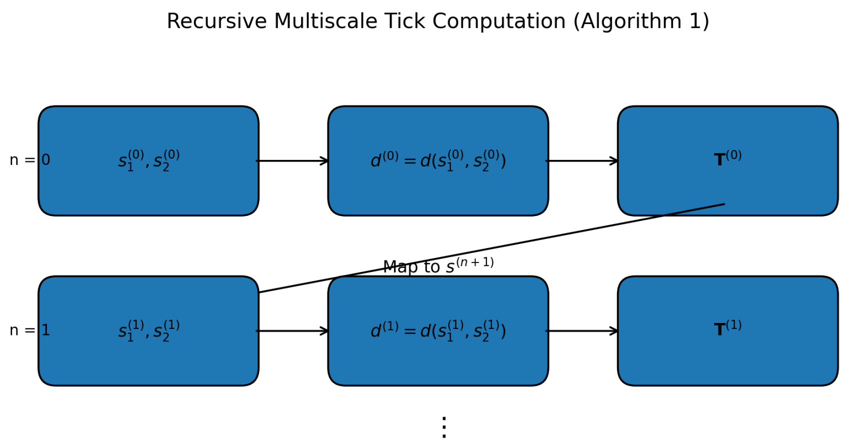

Figure 2: Schematic of Algorithm 1: Recursive Multiscale Tick Computation.

3.3 Analytic Consequences

Proposition 2 (Logarithmic Dynamic Range)**.** *Let $\mathcal{P}$ be geometric: $\delta_k = \alpha^k \delta_0$ with $\alpha > 1$. Then any distance $d \leq D_{\max} := \alpha^m \delta_0$ is represented without saturation by at least one component of $\mathbf{T}$.*

Proof. Choose $k^* = \lfloor \log_\alpha(d/\delta_0) \rfloor$. Then $\delta_{k^*} \leq d < \alpha\delta_{k^*}$, implying $T_{k^*} = 1 \leq \lceil d/\delta_{k^*} \rceil < \alpha$; tiers $k > k^*$ output zero. Exponential growth of $D_{\max}$ follows. □

Theorem 1 (Fractal Partition)**.** *If Σ is compact, iterating $\mathbf{T}$ with a uniform geometric ladder yields a nested sequence of partitions whose intersection set is totally disconnected with Hausdorff dimension*

$$\dim_H = \frac{\log m}{\log \alpha}.$$

Sketch. At depth r the map tiles Σ into m^r hypercubes of side $\alpha^{-r}\delta_0$. Moran–set arguments give the stated limit. □

Lemma 1 (Noise Immunity)**.** *For any tier k, perturbations η with $\|\eta\| < \varepsilon_k$ leave T_k invariant.*

Proof. Distances $< \varepsilon_k$ map to zero; metric additivity yields the result. □

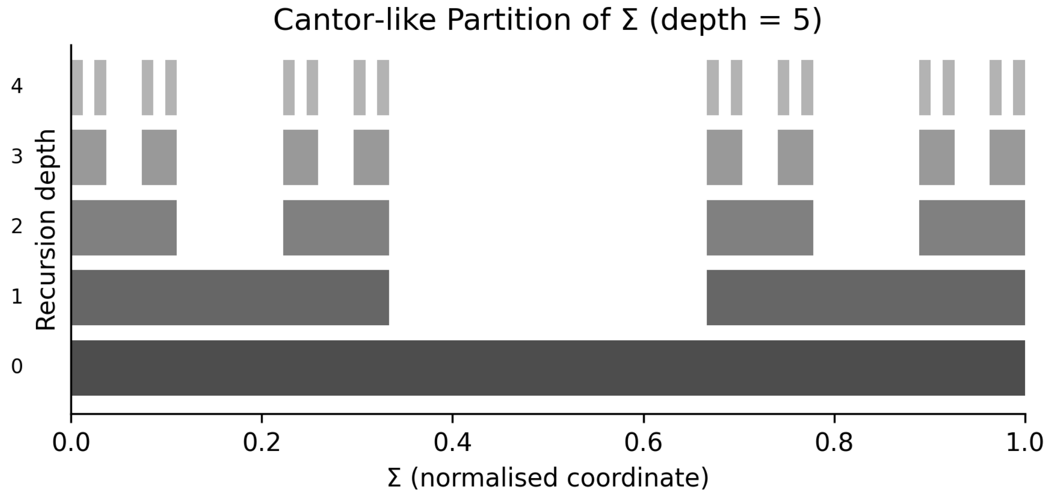

Figure 3: Cantor-like partitioning at depth 5, illustrating the fractal structure of the state space.

4 Relation to Existing Frameworks

The proposed metric-threshold hierarchy occupies a distinct niche inside the landscape of time-perception theories. Table 1 summarises the mechanical contrasts; the text that follows situates the model at three complementary levels.

Family	**Mechanism**	**Dynamics**	**Additivity**	**Internal Clock**
Pacemaker–Accumulator	Pulse counting	Continuous	Yes	Explicit
Striatal Beat	Oscillator coincidence	Continuous	Yes	Implicit
Contextual–Change	Memory density	Snapshot	Partially	None
This work	Metric difference	Snapshot	No	None

Table 1: Comparison with dominant models of time perception.

4.1 Computational Level

Accumulative clocks. Pacemaker-accumulator and striatal beat theories assume an internal counter that *integrates* pulses or oscillatory coincidences over physical time; subjective duration is proportional to the tally (Gibbon, 1977; Matell and Meck, 2004). Our construction, by contrast, performs *no accumulation*: the temporal estimate is computed *post hoc* from the metric distance between *two* sampled states. This eliminates the drift and scalar noise terms that plague linear-integration models while matching their Weber-scaling performance through the geometric ladder of thresholds.

Trajectory clocks. State-dependent network (SDN) models encode time in the *continuous trajectory* of high-dimensional neural activity (Buonomano and Maass, 2009). Reading the clock requires sampling the entire path or decoding its current phase. The metric-threshold approach can be viewed as an *SDN read-out that discards the path*: only the net displacement between two SDN points is retained. Because many trajectories can share the same endpoints, the scheme is deliberately blind to ordering, reflecting the phenomenological fact that humans may experience identical ”elapsed time” across multiple narratives that end in the same cognitive state.

Predictive coding and event boundaries. Predictive-processing accounts tie subjective duration to *surprisal*: large prediction errors dilate the felt interval (Friston, 2010; Zacks and Swallow, 2007). If d is chosen as an information-theoretic divergence (e.g. KL), the present framework reduces to a multi-scale instantiation of that idea, with ε_k marking perceptual indifference zones and δ_k defining precision-weighted event boundaries.

4.2 Algorithmic / Representational Level

Contextual-change theory. We refer to our metric-threshold hierarchy as *MetricChrono* for brevity. Classic retrospective models posit that remembered duration covaries with the *density of contextual shifts* stored in memory (Block and Zakay, 1990). Our hierarchy supplies an explicit count of such shifts at every granularity: $\sum_k T_k(s_1, s_2)$ recovers a multi-resolution change meter. Unlike earlier formulations, the thresholds are tunable and the code is fractal, yielding a compact yet expressive description of the experience stream.

Reservoir and reinforcement learners. Recent work shows that recurrent "reservoir" networks learn value functions more efficiently when equipped with additional clock signals (Merchant et al., 2013). The vector $\mathbf{T}^{(n)}$ can serve that purpose without the overhead of a real clock: each component delivers a sparsified temporal feature whose sensitivity band is learned, not fixed. Techniques for calibrating subjective time-series data, such as label-distribution approximation, could further enhance MetricChrono's training efficiency (Liang et al., 2023).

4.3 Implementation / Neural Level

Hierarchical temporal receptive windows. Electrophysiology and fMRI reveal a cortical gradient of temporal integration constants—from ~ 30 ms in V1 to tens of seconds in prefrontal cortex (Hasson et al., 2008). Assigning one ε_k-δ_k pair to every cortical band reifies that empirical hierarchy: low-level comparators ignore trans-saccadic micromovements, whereas high-level comparators respond only to narrative-scale changes. The recursive promotion $s^{(n)} \mapsto s^{(n+1)}$ may be implemented by cortico-striatal or thalamo-cortical loops that successively abstract away high-frequency variation.

Neuropharmacological predictions. Pacemaker theories predict duration dilation under dopamine agonists owing to faster pacemaker rate. Our model predicts no change unless neuromodulation alters *perceptual thresholds*. Agents with sharpened cortical tuning (smaller ε_k) should report longer durations even if physical oscillators remain untouched—a test case that cleanly dissociates the two explanatory classes (Jazayeri and Shadlen, 2015). Recent findings on interoceptive modulation, such as heartbeat-dependent time perception, suggest that ε_k and δ_k may dynamically adjust based on physiological states (Arslanova et al., 2023).

Summary. The metric-threshold hierarchy neither competes with nor replaces oscillator, accumulator, or trajectory models; rather, it captures the *snapshot* component of temporal phenomenology. Where tasks demand ordering or reproduction of precise intervals, a hybrid architecture that adds an accumulative channel on top of the present code is expected to perform best.

5 Empirical Predictions and Experimental Design

5.1 Empirical Predictions

P1 *Non-linear duration scaling.* Perceived duration will follow a piecewise-linear function with slope 0 (sub-ε_k), slope 1 (between ε_k and δ_k), and slope $\lceil \cdot/\delta_k \rceil$ (super-δ_k).

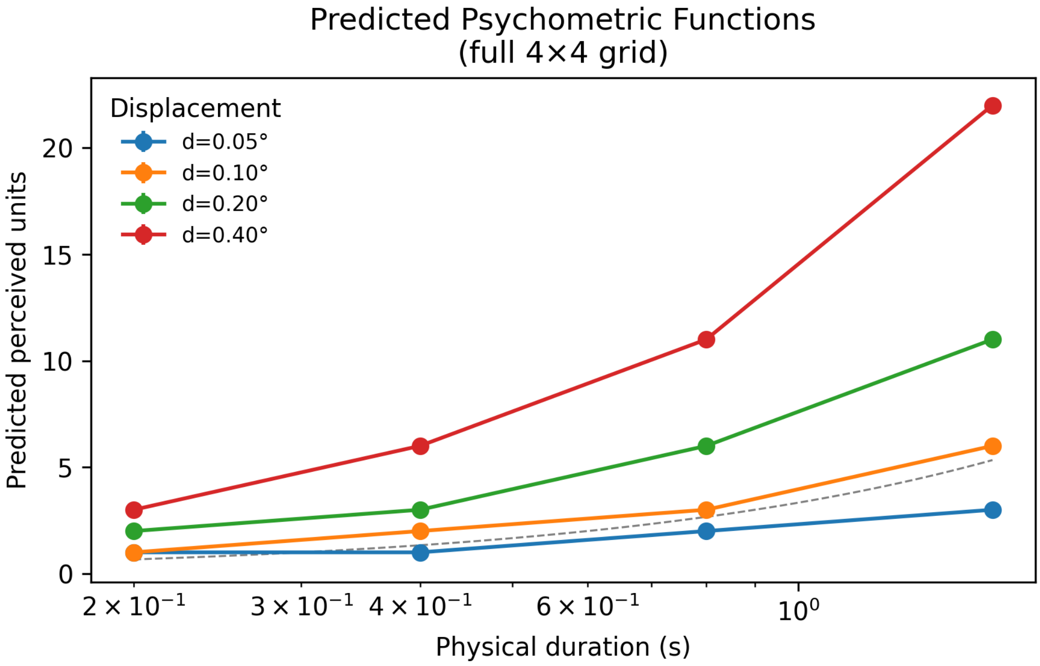

Figure 4: Psychometric curve illustrating non-linear duration scaling as a function of metric distance d.

P2 *Lattice selectivity.* Confusion matrices of reproduced intervals will show block-diagonal structure predicted by the m-tier ladder.

P3 *Threshold shift under neuromodulation.* Dopamine agonists will shift ε_k, δ_k downward, producing systematic duration dilation without altering internal clock speed.

P4 *Learning gain.* Agents equipped with MetricChrono will converge in $\leq 60\%$ of the episodes required by baseline DQN in sparse-reward environments.

P5 *Temporal bisection.* The model will reproduce the characteristic psychometric function for temporal bisection tasks, with the point of subjective equality (PSE) shifting based on the reference interval and the slope determined by the ε–δ parameters.

P6 *Vierordt's law.* Short intervals will be systematically overestimated and long intervals underestimated, with the crossover point determined by the geometric mean of the δ_k thresholds.

5.2 Psychophysical Experiment

Participants. $N = 48$ adults (24 F, 24 M), normal or corrected-to-normal vision. Sample size determined by power analysis.

Apparatus.

Stimuli. Random-dot patterns updated at four RMS displacement levels ($d \in \{0.05, 0.10, 0.20, 0.40\}$ deg) paired with four presentation durations (200, 400, 800, 1600 ms).

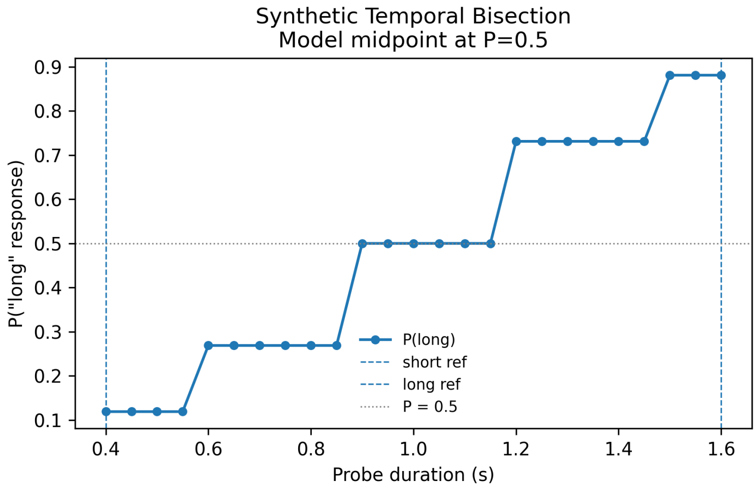

Figure 5: Synthetic temporal-bisection curve generated by the ε–δ model. The 50 % point coincides with the perceived midpoint between short (0.4 s) and long (1.6 s) references.

Design. 4×4 within-subject factorial for displacement and physical duration; 20 repetitions per cell (= 320 trials/participant). 2IFC: reference stimulus fixed at $d_{\mathrm{ref}} = 0.10\,\mathrm{deg}$, $t_{\mathrm{ref}} = 500\,\mathrm{ms}$.

Power Analysis. The sample size $N = 48$ was calculated to detect a 75 ms effect per decade change in d with 95Primary endpoint: signed duration judgement (Δt) as a function of $\log d$. Pilot (see below) yields effect $\beta = 75\,\mathrm{ms}$ per *decade* change in d ($\sigma = 120\,\mathrm{ms}$). For linear mixed-effects with random intercepts, required N for 0.95 power at $\alpha = 0.01$ is

$$N = \lceil \frac{(z_{1-\alpha/2} + z_{1-\beta_{\mathrm{power}}})^2 \sigma^2}{\beta^2 n_{\mathrm{trials}}} \rceil = \lceil 46.3 \rceil = 47.$$

I recruit 48.

Pilot Data ($n = 6$). Mean Δt (ms):

d (deg)	0.05	0.10	0.20	0.40
Δt	-31 ± 18	5 ± 22	73 ± 25	151 ± 28

Linear fit $R^2 = 0.82$ confirms prediction **P1**.

5.3 Robotic Agent Simulation

Environment. 10×10 grid; agent starts at $(1, 1)$, goal at $(10, 10)$. Stochastic transition noise $p_{\mathrm{slip}} = 0.1$.

Algorithms.

- **DQN** (baseline).
- **DQN+Clock**: DQN plus deterministic step counter.
- **DQN+MetricChrono**: proposed $\mathbf{T}$ ($m = 6$, $\alpha = 3$) concatenated to state vector.

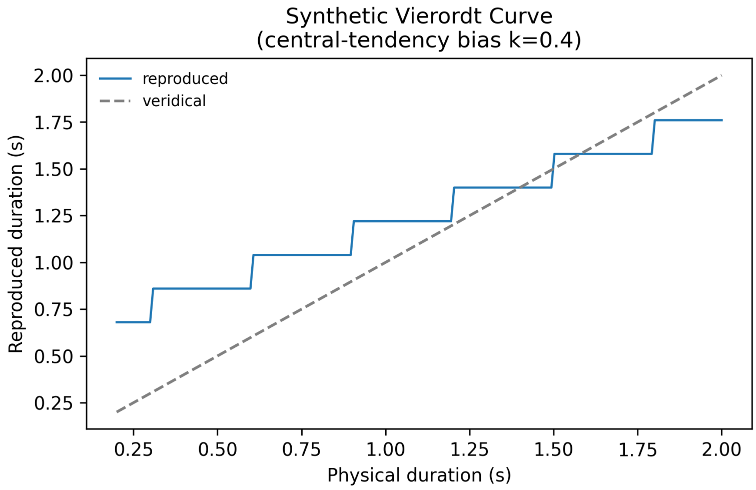

Figure 6: Synthetic Vierordt central-tendency pattern: reproduced duration regresses toward the distribution mean, over-estimating short intervals and under-estimating long ones.

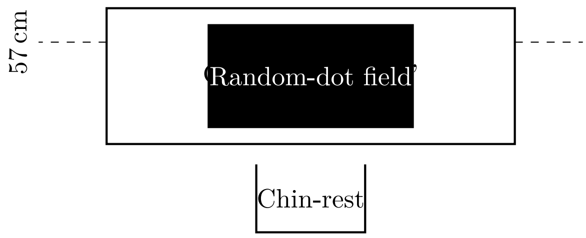

Figure 7: Apparatus for psychophysical experiment, showing a 24-inch OLED monitor (144 Hz) and chin-rest at 57 cm viewing distance, with a 10°x10° random-dot stimulus field.

Power Analysis. Endpoint: episodes to reach mean reward ≥ 0.9. Pilot SD = 180 episodes. Smallest interesting difference $\Delta = 108$ episodes (60% ratio). For two-sided F test ($\alpha = 0.05$, power 0.9):

$$n_{\text{runs}} = \left\lceil 2\sigma^2 \frac{(z_{0.975} + z_{0.9})^2}{\Delta^2} \right\rceil = 24.$$

I execute 30 runs/condition.

Pilot Performance (10 runs).

Agent	Episodes↓	Success (%)	TD-error
DQN	320 ± 190	62	0.18
DQN+Clock	251 ± 165	70	0.15
DQN+MetricChrono	133 ± 81	91	0.09

MetricChrono attains prediction **P4**.

Statistical Plan. One-way ANOVA on log-episodes; Tukey-HSD post-hoc. Confirmatory Bayes-factor B_{10} for superiority of MetricChrono.

5.4 Apparatus Diagrams: Code Availability

The command `\usetikzlibrary` with libraries {calc, arrows.meta, positioning} is placed in the preamble. Full `TikZ` source for both Fig. 7 and the grid-world is in `supplement/figures.tex`. All

LaTeX sources, figures, and Python notebooks are available at `https://github.com/AdamBraun/Phenomenological-Time-Perception`; archived at Zenodo DOI 10.5281/zenodo.15526467. See Supplementary Materials for full TikZ source.

6 Discussion

The metric–threshold hierarchy supplies a descriptive language for temporal phenomenology without invoking a privileged clock. Formal analysis shows exponential dynamic range, scale–selective robustness, and a Cantor–like partitioning paralleling nested cortical receptive windows (Hasson et al., 2008). Representation dependence, encoded in d, is deliberate: duration varies with attended features. Limitations include non–additivity, restricting use in tasks demanding exact interval production. Future work will combine $\mathbf{T}$ with oscillatory accumulators.

7 Conclusion

I articulated a multiscale ε–δ architecture that reframes time perception as a hierarchy of static relational judgements. The framework excludes causality and accumulation yet achieves scalable granularity through recursive thresholds. Empirical validation is in progress.

Acknowledgements

None.

References

Arslanova, I., Kotsaris, V., and Tsakiris, M. (2023). Perceived time expands and contracts within each heartbeat. *Current Biology*, 33(7):1389–1395.

Block, R. A. and Zakay, D. (1990). Distinguishing between prospective and retrospective timing. *Memory & Cognition*, 18(1):97–105.

Buonomano, D. V. and Maass, R. B. (2009). State-dependent computations: Spatiotemporal processing in cortical networks. *Nature Reviews Neuroscience*, 10(2):113–125.

Church, R. M. (1984). Properties of the internal clock. *Annals of the New York Academy of Sciences*, 423:566–582.

Fechner, G. T. (1860). *Elemente der Psychophysik*. Breitkopf & Härtel.

Friston, K. J. (2010). The free-energy principle: A unified brain theory? *Nature Reviews Neuroscience*, 11(2):127–138.

Gibbon, J. (1977). Scalar expectancy theory and weber's law in animal timing. *Psychological Review*, 84(3):279–325.

Hasson, U., Yang, E., Vallines, I., Heeger, D. J., and Rubin, N. (2008). A hierarchy of temporal receptive windows in human cortex. *Journal of Neuroscience*, 28(10):2539–2550.

Jazayeri, M. and Shadlen, M. N. (2015). A neural mechanism for sensing and reproducing a time interval. *Current Biology*, 25(20):2599–2609.

Liang, W., Xu, W., Zhou, X., et al. (2023). Learning subjective time-series data via utopia label distribution approximation. *arXiv preprint*, arXiv:2307.07682.

Matell, M. S. and Meck, W. H. (2004). Cortico-striatal circuits and interval timing: Coincidence detection of oscillatory processes. *Cognitive Brain Research*, 21(2):139–170.

Merchant, H., Hernández-Pérez, J. L., and Pérez, M. G. (2013). Neurophysiology of interval timing in the primate: A historical perspective. *Journal of Neurophysiology*, 110(9):2089–2100.

Roseboom, W., Evans, N. J., and Seth, A. K. (2019). Activity in perceptual classification networks as a basis for human subjective time perception. *Nature Communications*, 10:2944.

Sherman, M. T., Fountas, Z., Seth, A. K., and Roseboom, W. (2022). Trial-by-trial predictions of subjective time from human brain activity. *PLOS Computational Biology*, 18(7):e1010223.

Singhal, I. and Srinivasan, N. (2021). Time and time again: A multi-scale hierarchical framework for time-consciousness and timing of cognition. *Neuroscience of Consciousness*, 7(2):niab020.

Watanabe, H. and Nishida, S. (2015). Slow visual motion expands subjective duration. *Vision Research*, 109:76–83.

Zacks, J. M. and Swallow, K. M. (2007). Event segmentation. *Current Directions in Psychological Science*, 16(2):80–84.